Research Article

International Journal of Distributed Sensor Networks

International Journal of Distributed Sensor Networks
2020, Vol. 16(3)

DOI: 10.1177/1550147720908192
journals.sagepub.com/home/dsn
SAGE

Transverse deformation effect on sensitivity of strain-sensing patch antenna

Chunfeng Wan[1], Liyu Xie[2], Kangqian Xu[2], Songtao Xue[2,3], Can Jiang[2], Guochun Wan[4] and Tao Ding[5,6]

Abstract

The strain sensor based on microwave patch antenna is proposed to monitor structural strain in structural health monitoring. When patch antenna experiences deformation, the resonant frequency of patch antenna will shift. With these characteristics, the patch antenna can operate as both the strain-sensing element and communication component. This article chooses an RT-5880 rectangular patch antenna for strain measurement, focusing on its sensing performance. For distinguishing the influence of deformation in the antenna's length direction and width direction, the numerical simulation is implemented, and then two kinds of laboratory experiments are conducted. The first approach is to paste antennas in longitudinal and transverse ways and solve the equation set. The other approach is to design another patch antenna with narrow width and compare the test results with the wide one. All results show that the influence of deformation in wide direction on sensitivity can be neglected, and the resonant frequency shift has a good linear relationship with the strain of antenna in length direction.

Keywords

Structural health monitoring, strain sensor, patch antenna, resonant frequency

Date received: 11 July 2019; accepted: 29 January 2020

Handling Editor: Benny Lo

Introduction

The key members (e. g. joints or energy-consuming components) of structure may experience different degrees of damage after earthquake, hurricane, and flood. For example, the oil dampers installed on the first floor of the administration building of the Tohoku Institute of Technology were completely destroyed during the 2011 Great East Japan Earthquake.[1,2] When key members of structure destroy, the resistance to disaster of structure is weakened and even fatality happens unless the destroyed members would be repaired.[3] For ensuring the security of the structure and avoiding secondary disasters, the capability of the key members of the structure which experienced a disaster should be assessed and then decided whether to repair or substitute. In the process of assessment, as an important

[1]Southeast University, Key Laboratory of concrete and pre-stressed concrete structure of Ministry of Education, Nanjing, China
[2]Department of Disaster Mitigation for Structures, Tongji University, Shanghai, China
[3]Department of Architecture, Tohoku Institute of Technology, Sendai, Japan
[4]Department of Electronic Science and Technology, Tongji University, Shanghai, China
[5]MOE Key Laboratory of Advanced Micro-Structured Materials, Shanghai, China
[6]Institute of Precision Optical Engineering, School of Physics Science and Engineering, Tongji University, Shanghai, China

Corresponding author:
Liyu Xie, Department of Disaster Mitigation for Structures, Tongji University, Shanghai 200092, China.
Email: liyuxie@tongji.edu.cn

parameter of structure, strain is necessary to provide a reasonable reference. So it is useful to choose a suitable strain sensor to measure strain accurately and easily.

Traditional wired strain sensors include resistance strain gauge, vibrating wire strain gauges, and fiber Bragg optic sensors.[4] All of them require wires to supply power and transmit data, which is cost- and labor-consuming.[5] More fatally, when disaster happens, the strain sensors may fail due to the ruining of wires. To eliminate the wires in sensing system, many wireless strain sensors have been developed.[6–9] These devices usually contain a traditional strain-sensing element like the wired sensor for sensing strain, an analog-to-digital converter for converting strain data, a microprocessor for processing data, an antenna for transmitting data and a battery for supplying energy. These wireless sensors overcome the disadvantage of wired sensing system, but the sensing process requires multiple components cooperatively work, which makes sensing system complex and inefficient.

With the development of the interdisciplinary, some researchers have proposed sensors based on patch antenna which has a special property.[10,11] That is, when the patch antenna experiences deformation, the resonant frequency of the antenna changes accordingly, so the strain of patch antenna can be computed by measuring its resonant frequency. Based on this special property, the patch antenna can not only transmit data wirelessly but also work as the strain-sensing element. Furthermore, using the radiofrequency identification (RFID) technology, an RFID reader can wirelessly provide energy to an RFID tag[12] which contains a patch antenna and a chip. So working with a chip and an RFID reader, the antenna sensor can operate as a strain-sensing element, a data transmission element, and a power receiver simultaneously. Patch antenna, chip, and RFID reader constitute a simple and effective strain-sensing system which can measure strain wirelessly and passively. This system possesses good application prospects.

The patch antenna becomes the most critical module in the system due to its special property, and its strain-sensing characteristic is essential. There are a good linear relationship between the resonant frequency of patch antenna and the strain in its length direction according to the design formulas,[13–15] so patch antenna is very suitable as a strain-sensing element. With this property, scholars developed different sensors based on patch antenna and tested their sensing characteristics. Yi and colleagues[16,17] proposed a strain sensor based on rectangular patch antenna working at ultra-high frequency (UHF). Daliri et al.[18,19] presented a stain sensor based on circular patch antenna working at the microwave frequency. Zhao et al.[20] used in-phase quadrature (IQ) signal to improve the robustness of the antenna sensor. Other researches can be found in literature.[21–25]

The resonant frequency shift of patch antenna sensor under unit strain is defined as sensitivity coefficient, which will be affected by following aspects investigated before: (1) the efficiency of mechanical strain transferred from the base structure to the top surface of the antenna sensor due to shear lag effect;[26] (2) dielectric constant change of substrate caused by its deformation[27] and temperature.[28] Besides, the formula for designing patch antenna is based on transmission-line model,[29] in which the transverse alteration of electromagnetic fields is not taken into account. In other words, the influence of transverse deformation induced by Poisson effect on sensitivity of antenna sensor is neglected when antenna sensor experiences strain.

In order to ensure good linear relationship between resonant frequency of antenna sensor and strain in the length direction, the influence of deformation in the width direction on sensitivity should be discussed in case this simplified formula is not practical in strain monitoring. In this article, a chipless strain sensor based on RT-5880 rectangular patch antenna whose resonant frequency is around 2.45 GHz is proposed first. The tension experiments are carried out under the two conditions that the strain-sensing direction of chipped strain sensor is parallel to the tension direction and perpendicular to the tension direction, respectively. Then influence of the transverse strain can be decided by solving the equation set. In addition, another patch antenna with the same length and varying width of the former are designed. The influence of transverse deformation on sensitivity can be verified more intuitively by comparing the tension experiment results of the two patch antennas, so does the influence on initial resonant frequency.

The rest of the article is organized as follows. Section "Principle of operation" introduces the theory of strain-sensing mechanism of patch antenna. In section "Design and simulation of patch antenna," the patch antenna is modeled by finite-element software HFSS™, and its resonant frequency is simulated under the strain in length direction and width direction. In section "Experiments of patch antenna," two serial of experiments are designed to test the strain-sensing characteristics in both two directions. And section "Summary and discussion" provides a summary and discussion of this work.

Principle of operation

Rectangular patch antenna received considerable attention since 1970s, due to its advantages of compact-size, low profile, multiplexing, high gain, easy production, and so on. As antenna-enabled passive sensors for sensing temperature, strain, and other measurands, it has been studied extensively since the new millennium. The

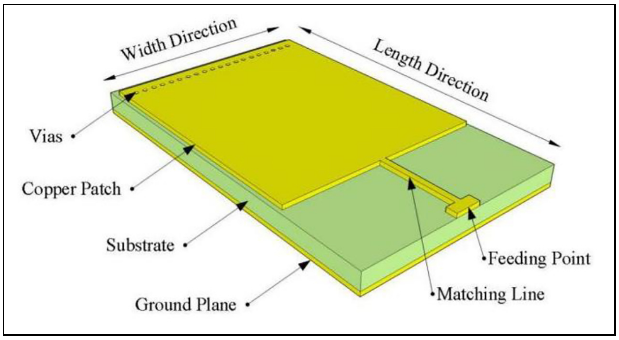

Figure 1. The components of quarter-wave rectangular patch antenna.

common rectangular patch antenna is a half-wavelength rectangular patch antenna.

The radiation patch could be folded by shorting the radiation patch and the ground plane through vias, reducing the antenna length of half-wavelength to quarter-wavelength. Thus, a quarter-wavelength rectangular patch antenna is adopted for sensing strain in this article.

As shown in Figure 1, the quarter-wavelength rectangular patch antenna consists of copper patch, ground plane, substrate, matching line, feeding point, and vias. The copper patch is the radiation source of electromagnetic wave. The substrate made of RT-5880 in this article is perforated at the top edge of copper patch, making the top copper patch and the bottom ground plane short-circuit with the vias. The antenna is connected with the load through the matching line and feeding point.

Transmission-line model of folded rectangular patch antenna

For analysis of microstrip antenna, the existing methods[30] are the transmission-line, cavity, and full wave. Among them, the transmission-line model renders good physical insight and is easy to apply, although it is less accurate. Basically, the microstrip antenna is modeled by two slots separated at a distance, ignoring the change of electromagnetic wave in width direction.

The resonant frequency of patch antenna which mainly depends on the length of the copper patch is the frequency at which power loss of patch antenna reaches minimum. In other words, the patch antenna will operate best when working at resonant frequency. At zero strain level, it can be calculated by the following formula[16]

$$f_{r0} = \frac{c}{4(L + \Delta L)\sqrt{\varepsilon_e}} \tag{1}$$

where f_{r0} is the initial resonant frequency, c is the speed of light, L is the length of the top copper patch, ε_e is the effective dielectric constant which can be estimated by relative dielectric constant ε_r as[31]

$$\varepsilon_e = \frac{\varepsilon_r + 1}{2} + \frac{\varepsilon_r - 1}{2}\sqrt{1 + \frac{10H}{W}} \tag{2}$$

where W is the width of the top copper patch, and H is the thickness of the substrate.

In formula (1), ΔL is the compensating additional length due to edge-fringing field defined in the following formula[32]

$$\Delta L = 0.412H\frac{(\varepsilon_e + 0.3)(W/H + 0.264)}{(\varepsilon_e - 0.258)(W/H + 0.8)} \tag{3}$$

According to these formulas, the resonant frequency of patch antenna is mainly dependent on the length of the top copper patch L, since ΔL is far less than L can be neglected.

When the antenna experiences strain ε_y in its length direction, the relationship between the resonant frequency f_r and the strain ε_y can be estimated as the following formula

$$f_r \approx \frac{c}{4(L + \Delta L)\sqrt{\varepsilon_e}(1 + \varepsilon_y)} = \frac{f_{r0}}{1 + \varepsilon_y} \tag{4}$$

Normally, the strain is far less than 1 and ΔL is far less than L in practice, which means formula (4) can be simplified as following formula

$$f_r \approx f_{r0} - f_{r0}\varepsilon_y \tag{5}$$

As can be seen in the formula (5), there is an approximately linear relationship between the resonant frequency of patch antenna and its strain in length direction, and the value of slope which represents the sensitivity coefficient of strain sensor is equal to the opposite number of initial resonant frequency. However, when the patch antenna experiences strain in length direction, its width change accordingly due to Poisson effect. On one hand, formula (1) based on transmission-line model ignores the change of electromagnetic wave in width direction. On the other hand, the compensating additional length and the change of effective dielectric constant are omitted which actually all varies with the width of patch antenna according to equations (2) and (3). In order to confirm the effect of intentional transverse deformation on sensitivity of patch antenna, the numerical simulation and experiments are conducted. Primarily, the measurement of resonant frequency of patch antenna should be introduced.

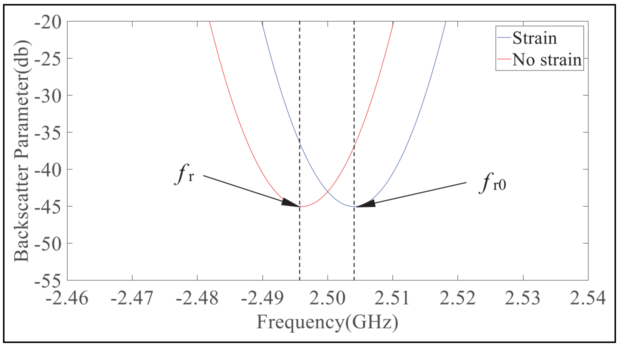

Figure 2. The measurement of the resonant frequency at different strain.

The measurement of the resonant frequency

The resonant frequency is measured by a network analyzer in this article. The electromagnetic wave is emitted by the network analyzer to patch antenna at different frequencies via a coaxial cable. Then the patch antenna reflects part of electromagnetic wave received back to the analyzer. The return loss $S_{11}(f)$ representing the degree of power loss can be estimated as the following formula

$$S_{11}(f) = 10\lg\left[\frac{P_{bs}(f)}{P_{em}(f)}\right] \tag{6}$$

where f is the frequency emitted by network analyzer, $P_{em}(f)$ is the input power, and $P_{em}(f)$ is the reflection power.

The return loss attains its minimum at the resonant frequency, since patch antenna losses the least energy when working at resonant frequency, as described in formula (7). So the resonant frequency of patch antenna can be obtained by searching the minimum of return loss curve. When patch antenna experiences strain, the curve will shift as the change of resonant frequency, shown in Figure 2. Then the changed resonant frequency can be obtained using the same method and the resonant frequency shift can be calculated

$$S_{11}(f_{r0}) = \min[S_{11}(f)] \tag{7}$$

Design and simulation of patch antenna

In this section, a finite-element software HFSS is used to design and simulate a quarter-wave rectangular patch antenna with RT-5880 substrate. In section "Patch antenna design," the patch antenna is designed. In section "Simulation of the patch antenna," simulation of patch antenna is implemented and the result is analyzed.

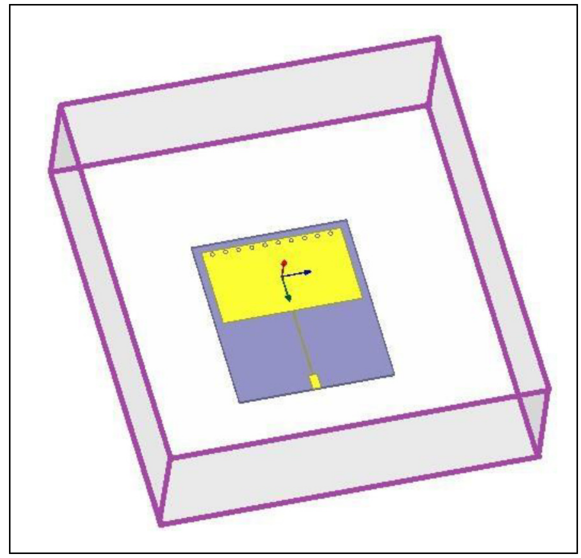

Figure 3. The HFSS model of the patch antenna.

Patch antenna design

Since a high sensitivity coefficient of chipless strain sensor needs a high initial resonant frequency of patch antenna according to formula (5), the patch antenna whose initial resonant frequency is around 2.45 GHz is chosen. The approximate size of patch antenna can be computed according to section "Principle of operation." Then the three-dimensional (3D) prototype of patch antenna is established in HFSS, as shown in Figure 3. The boundaries of copper patch and ground plane are set as perfect. The bonding between the copper patch/ground plane and the substrate are assumed to be ideal. The patch antenna is placed at the center of an air sphere. At the outer surface of the air sphere, only radiation is assigned.

In this model, the size of the matching line should be optimized, ensuring the impendence match between patch antenna and coaxial cable. In the case of impendence match, it is easiest for the network analyzer to measure the resonant frequency of patch antenna. The size parameters and dimensions of patch antenna models after optimizing are shown in Figure 4 and Table 1, respectively. Ultimately, the initial resonant frequency of patch antenna is solved by a frequency domain solver, and its value is 2.5269 GHz.

Simulation of the patch antenna

By increasing the length and decreasing the width of the patch antenna in HFSS, the uniaxial tension in the length direction of the patch antenna can be simulated. In this way, the resonant frequency of the patch antenna can be extracted from return loss curve solved

Table 1. The dimensions of patch antenna.

Parameters	W	L	H	W_1	W_2	L_1	L_2	L_3
Dimensions (mm)	39.0	45.4	0.5	35.0	2.1	20.6	18.7	4.0

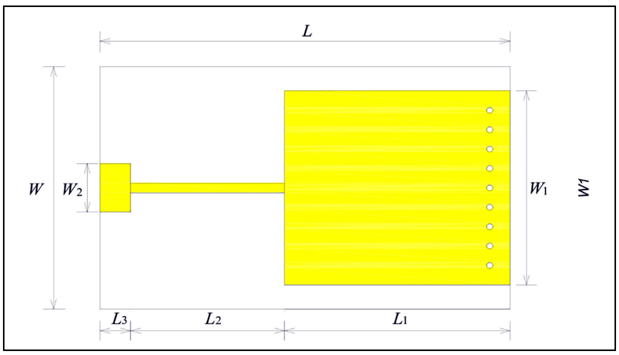

Figure 4. The parameters of patch antenna.

by HFSS under each strain level from 0‰ to 16‰ at an increment step of 2‰. As shown in Figure 5(a), the resonant frequency of patch antenna decreases as the tensile strain increases.

As shown in Figure 5(b), the correlation coefficient (R^2) is 0.9991, which means there is a good linear relationship between the resonant frequency of patch antenna and the strain in the length direction. The slope of fitted line is -2.4133 kHz/$\mu\varepsilon$, which represents the sensitivity coefficient of strain sensor, meaning the resonant frequency of patch antenna decreases 2.4133 kHz with 1 $\mu\varepsilon$ strain increments. According to formula (5), the theoretical value of the sensitivity coefficient should approximately equal to -2.5269 kHz/$\mu\varepsilon$, the opposite number of initial resonant frequency. The relative error between the simulated value and theoretical value is 4.50%, the reasons of which are as follows: (1) equation (5) is derived approximately and (2) the numerical simulation limits the accuracy since the change of the dimension is minor.

Experiments of patch antenna

In order to test the influence of deformation in width direction on sensitivity, two series of experiments are designed. The first experiments are designed in section "Design and results of Experiment I" by changing pasting method and its results are analyzed in section "Results analysis of Experiment I." Then a patch antenna whose width is narrower than former is designed for the other experiment in section "Design of Experiment II" and "Result analysis of Experiment II."

Design and results of Experiment I

The patch antennas are pasted on the aluminum plates, and the plates are loaded by a testing machine. The strain of plates is transferred to the antenna, which makes the resonant frequency of patch antenna shift. In order to test the influence of the deformation in two directions on sensitivity of patch antenna, it is necessary to measure the resonant frequency shift, the strain in the length direction and the strain in the width direction of patch antenna with deformation. But there are

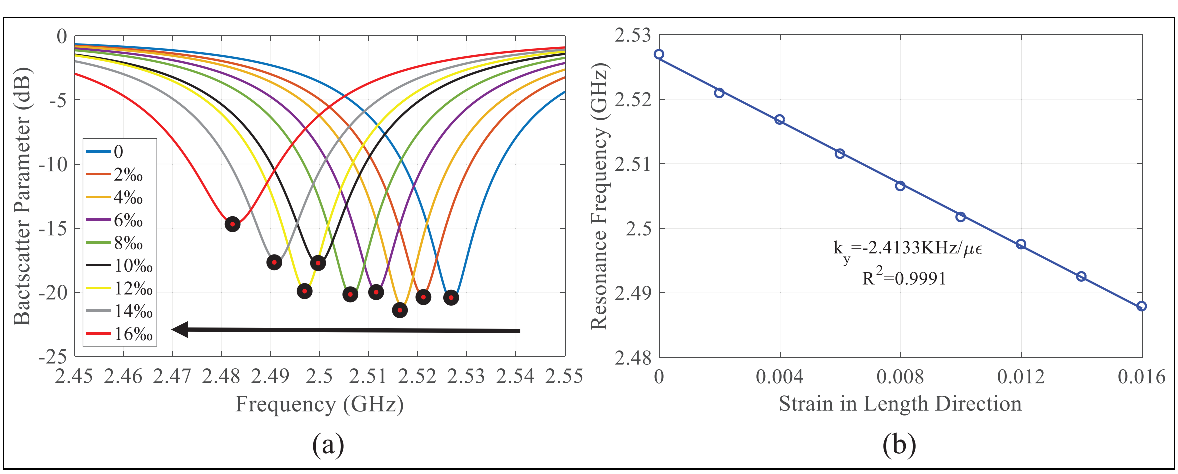

Figure 5. The simulation result when antenna experiment a strain in length direction: (a) the S_{11} curves at each strain level and (b) the relationship between the resonant frequency and the strain in length direction.

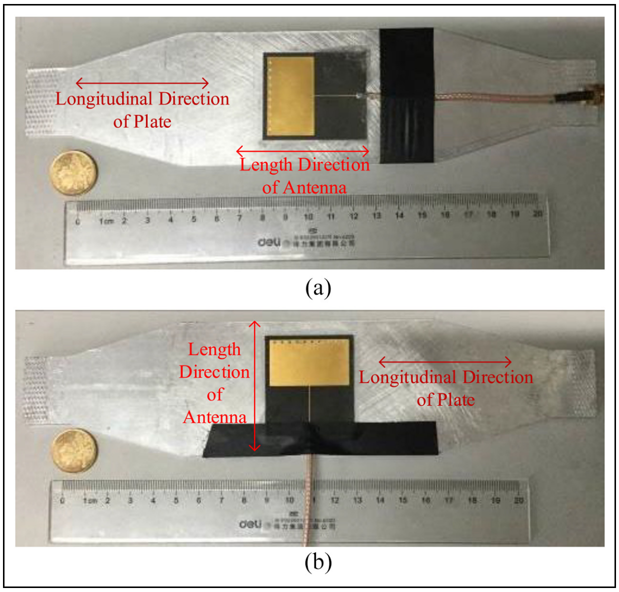

Figure 6. The experimental specimens of patch antenna: (a) In longitudinal way and (b) in transversal way.

two problems if those three parameters are measured directly.

1. Due to the Poisson effect, the strains in two directions (length and width) coexist at the same time when the patch antenna is under a uniaxial loading.
2. If the strain gauges are pasted on the antenna to measure the strain of antenna, the wires of strain gauges will disturb the electromagnetic field induced by patch antenna, causing an inaccurate measurement of the resonant frequency.

In order to avoid these problems, some indirect ways are adopted. For the strain measurement, a dynamometer is used to detect the tensile force of the testing machine (SJV-30000). Connected with the stiffness of the plates, the Poisson ratio of the plates and the strain transfer efficiency, the strain of antenna in both two directions can be calculated. To distinguish the influence of the strain in two directions, the antennas are pasted on the aluminum plates using super glue by two ways: the longitudinal way and the transversal way, as shown in Figure 6. The longitudinal way is that the length direction of antenna is parallel to the length direction of plate. And the transversal way is that the length direction of antenna is perpendicular to the length direction of plate. By pasting antennas in these ways, the strain of antenna on each antenna is different under the same tensile force applied to the two ends of plate, which causes a different resonant frequency shift. Then the influence of the strain in two directions can be distinguished by solving a binary linear equation group.

Table 2. The calculated results of transfer efficiency coefficient.

η_{22}	η_{12}	η_{11}	η_{21}
70.73%	85.26%	86.31%	79.19%

The experiment setup is designed as follows:

1. Carrying out an experiment study on aluminum plate characteristics, measuring the stiffness and the Poisson ratio of the plates.
2. Carrying out an experiment study on the strain transfer efficiency between the strain of patch antenna and plate.
3. Measuring the resonant frequency shift of the patch antennas pasted on the plates in longitudinal and transversal ways.

For the first experiment, using some wired strain gauges and a dynamometer, the tensile force and the strain of aluminum plate in both longitudinal and transversal directions can be measured. Then the stiffness and Poisson ratio of aluminum plate can be computed. Repeating the experiment three times, the average of measured stiffness K is 68.5 GPa and the average of measured Poisson ratio μ is 0.331.

For the second experiment, the strain of plate and the strain of antenna in both two directions are measured with some strain gauges. The strain transfer efficiency coefficients η_{22}, η_{12}, η_{11}, and η_{21} can be calculated using formula (8)

$$\begin{cases} \eta_{22} = \frac{\varepsilon_{ANy}}{\varepsilon_{PLy}}, \ \eta_{12} = \frac{\varepsilon_{ANx}}{\varepsilon_{PLx}} \ \text{(in longitudinal way)} \\ \eta_{11} = \frac{\varepsilon_{ANx}}{\varepsilon_{PLx}}, \ \eta_{21} = \frac{\varepsilon_{ANy}}{\varepsilon_{PLy}} \ \text{(in transversal way)} \end{cases} \tag{8}$$

where η is the strain transfer efficiency coefficient. The first subscript represents the direction of the transfer efficiency. "1" represents the width direction of patch antenna, and "2" represents the length direction of patch antenna. The second subscript represents the pasting way. "1" represents the transversal way, and "2" represents the longitudinal way. ε_{ANy} is the strain of patch antenna in the length direction, ε_{ANx} is the strain of patch antenna in the width direction, ε_{PLy} is the strain of aluminum plate in the length direction, and ε_{PLx} is the strain of aluminum plate in the width direction. Besides, here is the relationship $\varepsilon_{PLx} = -\mu\varepsilon_{PLy}$.

The test results of transfer efficiency coefficients are recorded in Table 2.

The setup of the third experiment is shown in Figure 7. The dynamometer is used to measure the tensile force, and the network analyzer is used to detect

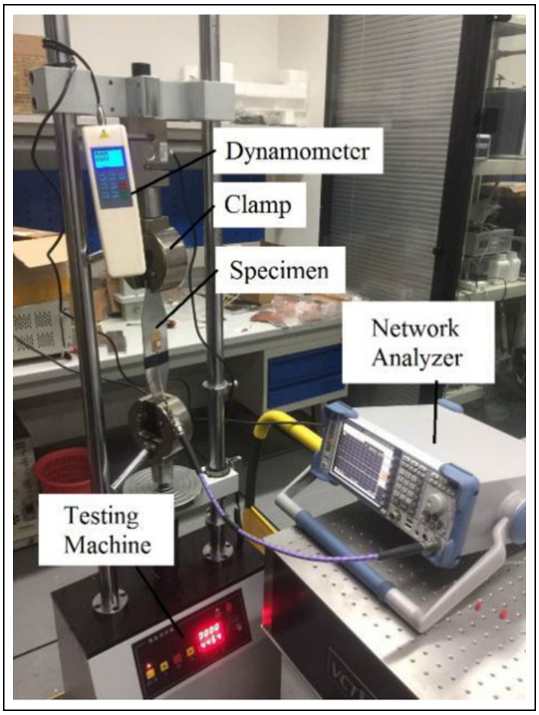

Figure 7. The setup of loading experiment.

the resonant frequency of patch antenna. The testing machine loads from 0 kN to around 12 kN with an increment step of 2 kN. The longitudinal strain of the aluminum plate reaches around 700 με when the loading process is completed.

At each load level, the network analyzer records the S_{11} curve 10 times, and these curves are averaged as follows

$$S_{11}(f) = \frac{1}{10}\sum_{i=1}^{10} S_{11,i}(f) \quad (9)$$

The load step is 2 kN, which causes only 120 με strain increment. So the averaged return loss curves of two adjacent steps are very close. In order to demonstrate the tendency of return loss curve shift clearly, the return loss curve (antenna pasted in longitudinal way) at every three step are shown in Figure 8(a). Obviously, there is a decreased tendency of resonant frequency of patch antenna when the tensile force increases. Due to the environment noise, the return loss curves are very rough, which makes the extraction of resonant frequency more difficult. As shown in Figure 8(b), a quadratic polynomial is adopted to fit the bottom of the return loss curve, and the minimum point of the fitted polynomial is chosen as the resonant frequency of patch antenna. By this method, the initial resonant frequency, 2.5209 GHz, is detected.

After extracting the resonant frequency of patch antenna at each load level, the relationship between the resonant frequency of patch antenna and the longitudinal strain of the aluminum plate is fitted linearly. This experiment is repeated three times, and the results of the first time are shown in Figure 9. Figure 9(a) show the result of specimen pasted in longitudinal way, and Figure 9(b) shows the result of specimen pasted in transverse way. In these figures, the abscissas present the longitudinal strain of the plates, which can be computed with the tensile force and the stiffness of the plates. When patch antenna is pasted in the longitudinal way, the resonant frequency of patch antenna decreases resulting from the increasing tensile force. In the situation of pasting patch antenna in transversal way, the resonant frequency of patch antenna increases as the load increases because of the compression strain of patch antenna in the length direction caused by Poisson effect.

After completing each experiment three times, the average slope of fitted line and the longitudinal strain

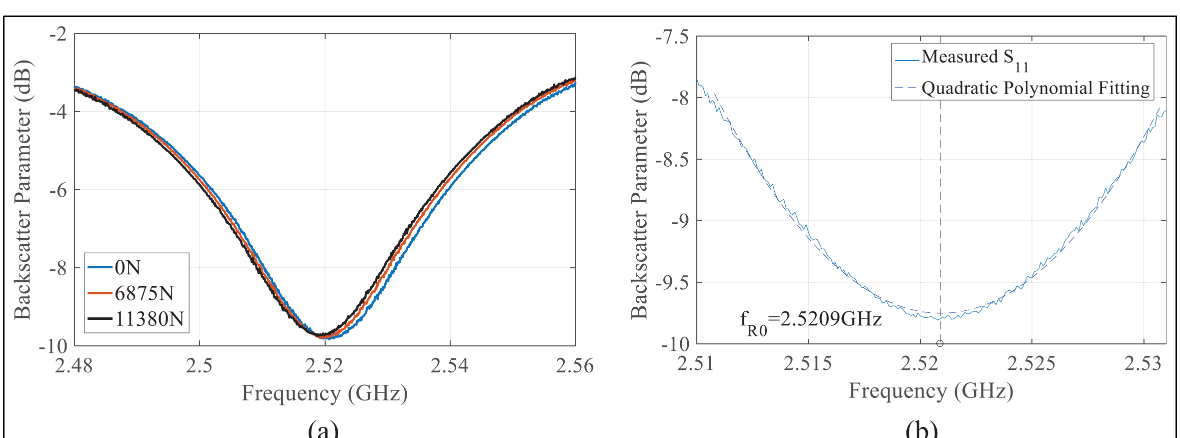

Figure 8. The tested return loss curves (longitudinal pasting way): (a) S_{11} curves at different load levels and (b) quadratic polynomial of S_{11} curves.

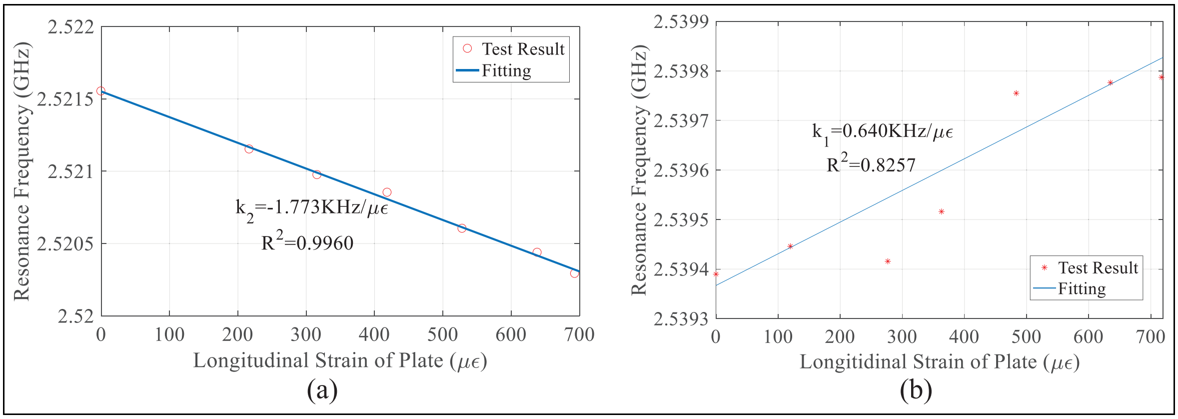

Figure 9. The relationship between the resonant frequency and the longitudinal strain of plate: (a) pasting antenna in longitudinal way and (b) pasting antenna in transversal way.

are calculated. When the patch antenna is pasted in longitudinal way, the averaged slope k_2 is -1.730 kHz/$\mu\varepsilon$. And when the patch antenna is pasted in transverse way, the averaged slope k_1 is 0.689 kHz/$\mu\varepsilon$.

Results analysis of Experiment I

Due to the coexistence of the plate's strain in two directions, the influence of the strain in length and width direction on sensitivity of patch antenna should be decomposed. The strain of patch antenna in length and width direction can be computed with the longitudinal strain of plate ε_{PLy}, the strain transfer efficiency coefficient η, and Poisson ratio of plate μ as shown in the following equation

$$\varepsilon_{ANy} = \begin{cases} \eta_{22}\varepsilon_{ALy}, & \text{in longitudinal way} \\ -\mu\eta_{21}\varepsilon_{ALy}, & \text{in transversal way} \end{cases}$$
$$\varepsilon_{ANx} = \begin{cases} -\mu\eta_{12}\varepsilon_{ALy}, & \text{in longitudinal way} \\ \eta_{11}\varepsilon_{ALy}, & \text{in transversal way} \end{cases} \quad (10)$$

For a longitudinally pasted antenna, when the longitudinal strain of the aluminum plate is ε_{PLy}, the resonant frequency shift is $k_2\varepsilon_{PLy}$ according to section "Results analysis of Experiment I." According to formula (10), the strain of patch antenna in length direction is $\eta_{22}\varepsilon_{ALy}$, which causes the resonant frequency shift $k_y\eta_{22}\varepsilon_{ALy}$, where k_y represents the sensitivity coefficient of chipless strain sensor corresponding to the strain of patch antenna in length direction; the strain in width direction is $-\mu\eta_{12}\varepsilon_{ALy}$, which causes the resonant frequency shift $-k_x\mu\eta_{12}\varepsilon_{ALy}$, where k_x represents the sensitivity coefficient of chipless strain sensor corresponding to the strain of patch antenna in width direction. Similarly, for a transversally pasted antenna, when the longitudinal strain of the plate is ε_{PLy}, and the resonant frequency shift is $k_1\varepsilon_{PLy}$. The strain of patch antenna in length direction is $-\mu\eta_{21}\varepsilon_{ALy}$, which causes the resonant frequency shift $-k_y\mu\eta_{21}\varepsilon_{ALy}$; the strain in width direction is $\eta_{11}\varepsilon_{ALy}$, which causes the resonant frequency shift $k_x\eta_{11}\varepsilon_{ALy}$. Then, formula (11) can be inferred as

$$\begin{cases} k_2 = \eta_{22}k_y - \mu\eta_{12}k_x \\ k_1 = -\mu\eta_{21}k_y + \eta_{11}k_x \end{cases} \quad (11)$$

By solving this equation set, the slope k_y is -2.4739 kHz/$\mu\varepsilon$, which is very close to the initial resonant frequency of the patch antenna. And k_x is -0.0062 kHz/$\mu\varepsilon$, showing the strain in the width direction has very little effect on sensitivity. In other words, the influence of the deformation in the width direction on sensitivity of patch antenna can be ignored.

Design of Experiment II

In this section, another patch antenna whose dimensions are the same with the one in front except the width is designed. On one hand, the influence on initial resonant frequency can be researched induced by width change. On the other hand, when the two kinds of patch antennas are stretched longitudinally with the deformation in length direction, their transverse deformation are different due to the varying width, so the influence of the transverse deformation on sensitivity of patch antenna can be verified by tension experiments.

According to the formulas in section "Principle of operation," the narrow patch antenna is designed. The process of design is similar to the one in the front. The parameters and dimensions of the narrow patch antenna are shown in Figure 4 and Table 3.

Then the tension experiments of the two kinds of patch antennas are conducted. They are bonded on the aluminum plates for stretching, respectively, shown in Figure 10. The axial force applied is applied at the two

Table 3. The dimensions of narrow patch antenna.

Parameters	W	L	H	W_1	W_2	L_1	L_2	L_3
Dimensions (mm)	21.0	45.4	0.5	17.0	2.1	20.6	18.7	4.0

Table 4. The experiment results of two kinds of patch antennas.

Sample	The initial resonant frequency (GHz)	Measured sensitivity (GHz/ε)	The ratio	Longitudinal transfer efficiency	Relative error
Wide patch antenna	2.522	1.777	70.46%	70.73%	0.38%
Narrow patch antenna	2.372	1.793	75.59%	76.44%	1.11%

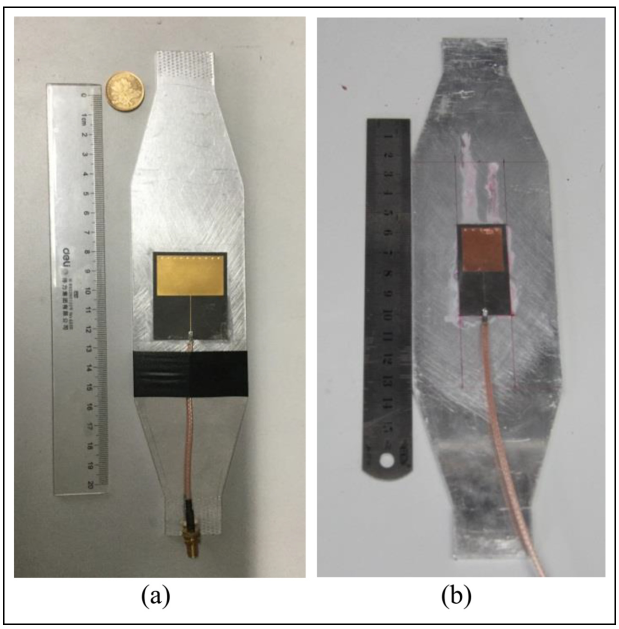

Figure 10. Experimental specimens of patch antenna: (a) the wide antenna specimen and (b) the narrow antenna specimen.

ends of specimen from 0 to 12 kN at an approximate increment step of 2 kN by the tensile testing machine so that different strain levels from 0 to 700 $\mu\varepsilon$ approximately can be generated in the specimen.

Result analysis of Experiment II

At each strain level, the return loss curve is obtained by network analyzer and the resonant frequency of patch antenna is extracted from the return loss curve by picking its minimum. Then the resonant frequency shift is fitted linearly with respect to the applied strain of plate in the length direction. The results are shown in Figure 11 and Table 4.

The measured initial resonant frequency of the wide patch antennas is 2.522 GHz, and the measured

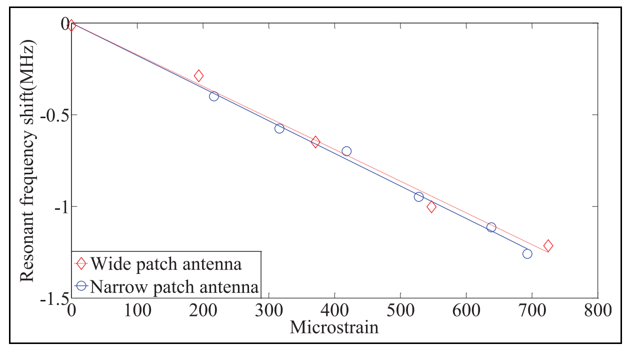

Figure 11. Strain-resonant frequency-fitted lines.

sensitivity coefficients of chipless strain sensor which is equal to the slope of the fitted line is –1.777 kHz/$\mu\varepsilon$. For narrow patch antenna, the two parameters are 2.372 GHz and –1.793 kHz/$\mu\varepsilon$, respectively. Due to the difference between initial resonant frequencies of the two kinds of patch antennas, the ratio of the measured sensitivity coefficients to initial resonant frequencies is used to compare between them, which are 0.7046 and 0.7559, respectively. According to sections "Principle of operation" and "Experiments of patch antenna", the value of the ratio should be equal to the transfer efficiency coefficient η_{22}, whose value is 70.73% for wide patch antenna and 76.44% for narrow patch antenna. The relative error for the two antennas are 0.38% and 1.11%, respectively. So the experiment results indicate that the initial resonant frequency of patch antenna will be affected due to the change of width, but the influence of the transverse deformation on sensitivity of patch antenna can be neglected in engineering.

Summary and discussion

This article designs and manufactures the RT-5880 quarter-wave rectangular patch antenna as a strain sensor and focuses on the sensing performance. According to the design formula of the patch antenna, it has a good unidirectivity of strain-sensing characteristic, but the design formula is based on the transmission-line model which ignores the influence of deformation in width direction to simplify the model. So simulations and experiments are conducted to study on the influence of deformation in both two directions on sensitivity of patch antenna. The results show that the deformation in width direction has a very little influence on sensitivity of patch antenna, which means the chipless strain sensor has a good linear relationship between the resonant frequency of patch antenna and the strain in length direction. Therefore, the patch antenna has good strain-sensing characteristics as a strain sensor.

This antenna sensor still needs coaxial cable for power supply and data transmission. However, the patch antenna shows good strain-sensing characteristics, so it can be used to form an RFID strain-sensing system with a chip and RFID reader, making wireless detection realized. In this system, the patch antenna operates as strain-sensing element, data transmission element, and power receiver simultaneously, which simplifies the wireless strain-sensing system and improves its efficiency. So as a new strain-sensing element, the patch antenna has a board prospects.

Declaration of conflicting interests

The author(s) declared no potential conflicts of interest with respect to the research, authorship, and/or publication of this article.

Funding

The author(s) disclosed receipt of the following financial support for the research, authorship, and/or publication of this article: This study was supported by the Key Program of Intergovernmental International Scientific and Technological Innovation Cooperation (grant no. 2016YFE0127600), Key Laboratory of Performance Evolution and Control for Engineering Structures (Tongji University), Ministry of Education (grant no. 2018KF-4), and the Fundamental Research Funds for the Central Universities.

ORCID iD

Kangqian Xu https://orcid.org/0000-0002-6198-3982

Reference

1. Cao M, Tang H, Funaki N, et al. Study on a real 8F steel building with oil damper damaged during the 2011 Great East Japan earthquake. In: *Proceedings of 15th world conference on earthquake engineering*, Lisbon, 24–28 September 2012, pp. 1–10.
2. Xie L, Cao M, Funaki N, et al. Performance study of an eight-story steel building equipped with oil dampers damaged during the 2011 great east Japan earthquake part 1: structural identification and damage reasoning. *J Asian Architect Build Eng* 2015; 14: 181–188.
3. Ou J. Intelligent monitoring and health diagnosis of major engineering structures. *Eng Mech* 2002; 2002: 1–12.
4. Zhou Y, So R, Jin W, et al. Dynamic strain measurements of a circular cylinder in a cross flow using a fibre Bragg grating sensor. *Exp Fluids* 1999; 27: 359–367.
5. Celebi M. *Seismic instrumentation of buildings*. USGS Open File Report 00-157, US Department of the Interior, US Geological Survey, April 2000.
6. Straser EG, Kiremidjian AS, Meng TH, et al. Modular 2001 wireless damage monitoring system for structures: No. 6,292,108.
7. Spencer Jr BF , Ruiz Sandoval ME and Kurata N. Smart sensing technology: opportunities and challenges. *Struct Control Health Monit* 2004; 11: 349–368.
8. Lynch JP, Law KH, Kiremidjian AS, et al. Design and performance validation of a wireless sensing unit for structural monitoring applications. *Struct Eng Mech* 2004; 17: 393–408.
9. Wang Y, Lynch JP and Law KH. A wireless structural health monitoring system with multithreaded sensing devices: design and validation. *Struct Inf Eng* 2007; 3: 103–120.
10. Rao KS, Nikitin PV and Lam SF. Antenna design for UHF RFID tags: a review and a practical application. *IEEE T Antenna Propag* 2005; 53: 3870–3876.
11. Rida A, Yang L and Tentzeris MM. *RFID-enabled sensor design and applications*. Dedham, MA: Artech House, 2010.
12. Finkenzeller K. *RFID handbook: fundamentals and applications in contactless smart cards, radio frequency identification and near-field communication*. Hoboken, NJ: John Wiley & Sons, 2010.
13. Deschamps GA and Sichak W. Microstrip microwave antennas. In: *Proceedings of 3rd USAF symposium on antennas*, Champaign, IL, 18–22 October 1953.
14. Munson R. Conformal microstrip antennas and microstrip phased arrays. *IEEE T Antenna Propag* 1974; 22: 74–78.
15. Garg R, Bhartia P, Bahl IJ, et al. *Microstrip antenna design handbook*. Dedham, MA: Artech House, 2001.
16. Yi X, Wu T, Wang Y, et al. Passive wireless smart-skin sensor using RFID-based folded patch antennas. *Int J Smart Nano Mater* 2011; 2: 22–38.
17. Yi X, Cho C, Cooper J, et al. Passive wireless antenna sensor for strain and crack sensing—electromagnetic modeling, simulation, and testing. *Smart Mater Struct* 2013; 22: 85009.
18. Daliri A, Galehdar A, John S, et al. Circular microstrip patch antenna strain sensor for wireless structural health monitoring. In: *Proceedings of the world congress on engineering*, London, 30 June–2 July 2010, http://www.iaeng.org/publication/WCE2010/WCE2010_pp1173-1178.pdf
19. Daliri A, Galehdar A, John S, et al. Wireless strain measurement using circular microstrip patch antennas. *Sensors Actuator A: Phys* 2012; 184: 86–92.
20. Zhao A, Tian GY and Zhang J. IQ signal based RFID sensors for defect detection and characterisation. *Sensors Actuator A: Phys* 2018; 269: 14–21.

21. Bai L. *RFID sensor-driven structural condition monitoring integrated building information modeling environment*. PhD thesis, Department of Civil Engineering, University of Maryland, College Park, MD, 2013.
22. Huang H. Flexible wireless antenna sensor: a review. *IEEE Sens J* 2013; 13: 3865–3872.
23. Sanders JW, Yao J and Huang H. Microstrip patch antenna temperature sensor. *IEEE Sens J* 2015; 15: 5312–5319.
24. Ozbey B, Erturk VB, Demir HV, et al. A wireless passive sensing system for displacement/strain measurement in reinforced concrete members. *Sensors* 2016; 16: 496.
25. Xue S, Xu K, Liyu X, et al. Crack sensor based on patch antenna fed by capacitive microstrip lines. *Smart Mater Struct* 2019; 28: 8.
26. Tata U, Huang H, Carter RL, et al. Exploiting a patch antenna for strain measurements. *Meas Sci Technol* 2008; 20: 15201.
27. Yi X, Wu T, Wang Y, et al. Sensitivity modeling of an RFID-based strain-sensing antenna with dielectric constant change. *IEEE Sens J* 2015; 15: 6147–6155.
28. Tchafa FM and Huang H. Microstrip patch antenna for simultaneous strain and temperature sensing. *Smart Mater Struct* 2018; 27: 65019.
29. Bahl IJ and Bhartia P. *Microstrip antennas*. Dedham, MA: Artech house, 1980.
30. Constantine AB. *Antenna theory: analysis and design: microstrip antennas*. 3rd ed. Hoboken, NJ: John Wiley & Sons, 2005.
31. Balanis CA. *Advanced Engineering Electromagnetics*. 2nd ed. Hoboken, NJ: John Wiley & Sons, 2012.
32. Hammerstad EO. Equations for microstrip circuit design. In: *Proceedings of the IEEE 5th European microwave conference*, Hamburg, 1–4 September 1975. New York: IEEE.